Available online at www.sciencedirect.com
SCIENCE DIRECT®
Chemical Physics Letters 402 (2005) 175–179
CHEMICAL PHYSICS LETTERS
www.elsevier.com/locate/cplett

Investigation of the highest occupied molecular orbital of propene by binary (e, 2e) spectroscopy

C.G. Ning, X.G. Ren, J.K. Deng *, S.F. Zhang, G.L. Su, H. Zhou, B. Li, F. Huang, G.Q. Li

Department of Physics, Building of School of Science, Tsinghua University, Beijing 100084, PR China

Received 11 October 2004; in final form 3 December 2004
Available online 22 December 2004

Abstract

We report here the first measurements of the momentum profile of highest occupied molecular orbital (HOMO) and the complete valence shell binding energy spectra of propene with impact energies of 600 and 1200 eV by a binary (e, 2e) spectrometer. The experimental momentum profile of the HOMO orbitals was compared with the theoretical momentum distributions calculated using Hartree–Fock and density functional theory methods with various basis sets. The discrepancy between experimental and theoretical data was explained using the distorted wave effects.

1. Introduction

Electron momentum spectroscopy (EMS), based on a binary (e, 2e) ionization reaction, has been shown to be a powerful and informative experimental tool for study of the electronic structure of atoms, molecules, biomolecules and condensed matter [1–3]. EMS can access the complete valence shell binding energy range, though with lower energy resolution than in most photo electron spectroscopy (PES). In particular, the unique ability of EMS to measure electron momentum distributions of individual molecular orbitals has made it become an important experimental technique for study of electronic structures in atoms, molecules and solids. The frontier orbital HOMO is very important for many chemical and physical properties. In other studies of structure–reactivity relations and molecular similarity and dissimilarity studies, Cooper and Allan [4] suggested that it would be interesting and potentially fruitful if momentum space was calculated on a HOMO/LUMO (the lowest unoccupied molecular orbital) orbital rather than a total density basis. Our experimental result and related theoretical investigation for propene provided the details of the HOMO electron density distributions information in momentum space.

Study of the electronic structure of small saturated and unsaturated hydrocarbon molecules has received much interest [5–7]. As the simplest straight chain hydrocarbon molecule that has both carbon–carbon double bond and carbon–carbon single bond, propene, C_3H_6, serves as an excellent prototype of model alkene. In addition to its fundamental interest in quantum chemistry, propene is also an important raw material for reagent compound synthesis and polymer production. The electronic states of propene were extensively investigated by various experimental and theoretical methods [8–11]. The equilibrium conformation of propene has C_s point group symmetry.

In this Letter, we report the first complete valence shell binding energy spectra (BES) (8–37 eV) of propene and its HOMO electron momentum profile using EMS at an impact electron energy of 1200 and 600 eV plus binding energy with a symmetric non-coplanar geometry. The

* Coresponding author. Fax: +86 10 6278 1604.
E-mail address: djk-dmp@mail.tsinghua.edu.cn (J.K. Deng).

0009-2614/$ - see front matter © 2004 Elsevier B.V. All rights reserved.
doi:10.1016/j.cplett.2004.12.020

experimental momentum profile is compared with Hartree–Fock (HF) and density functional theory (DFT) calculations using various basis sets. The discrepancy between experiment and theory is explained qualitatively through the distorted wave effects.

2. Methods

Recently, we have developed a new type of EMS spectrometer with two orders higher efficiency than our previous one [12]. The basic principle of EMS is ionization reaction initiated by electron beam. The gas phase target molecules are ionized by impact with a high energy electron beam. The outgoing electrons (scattered and ionized) are angle and energy selected by a toroidal energy analyzer and then detected in coincidence. The experimental geometry is symmetric non-coplanar, that is the two outgoing electrons are selected to have equal polar angles ($\theta_1 = \theta_2 = 45°$, angle between the outgoing electron direction and the incoming electron beam direction). The azimuthal angles (ϕ, angle between the two outgoing electron directions in the plane normal to the beam direction and $\phi = 0$ is the scattering plane) from $-38°$ to $38°$ are simultaneously measured, which is the significant improvement compared with our previous spectrometer which only collects the (e, 2e) events at a fixed ϕ angle one time. A profile of differential cross-section versus recoil momentum for each energy resolved state of the target molecules can be obtained from these BES at different ϕ angles. Under the binary encounter requirements of high impact energy, high momentum transfer and negligible kinetic energy transfer to the residual ion, the initial momentum p of the knocked-out electron can be shown by

$$p = \left\{ (2p\cos\theta_1 - p_0)^2 + [2p_1 \sin\theta_1 \sin(\phi/2)]^2 \right\}^{1/2}, \quad (1)$$

where p_1, p_2 ($p_1 = p_2$) are the momentum of each of the two outgoing electron and p_0 is the momentum of the incident electron.

The EMS binary (e, 2e) differential cross-section under the plane wave impulse approximation (PWIA) for randomly oriented gas-phase molecules is given by [1]

$$\sigma_{\mathrm{EMS}} \propto \int \frac{\mathrm{d}\Omega}{4\pi} \left| \left\langle p\Psi_f^{N-1} \mid \Psi_i^N \right\rangle \right|^2, \quad (2)$$

where p is the momentum of the target electron prior to the electron ejection. $|\Psi_i^N\rangle$ and $|\Psi_i^{N-1}\rangle$ are the total electronic wave functions for the final ion state and the target molecule ground (initial) state, respectively. Under the target Hartree–Fock approximation (THFA), the EMS cross-section can be simplified by [3,13]

$$\sigma_{\mathrm{EMS}} \propto \mathrm{S}_j^f \int \mathrm{d}\Omega \left|\psi_j(p)\right|^2, \quad (3)$$

where $|\psi_j(p)\rangle$ is the independent-particle momentum space wavefunction for the jth electron that was ionized. S_j^f is called spectroscopic factor or pole strength. The integral in Eq. (3) is known as the spherically averaged one-electron momentum distribution (MD). Therefore, EMS has the ability to image the electron density distribution in individual orbitald selected according to their binding energies.

In EMS, the individual orbitals are selected by the binding (or ionization) energy. With the multi-channel energy dispersive spectrometer used in the present Letter, BES are collected at various azimuthal angles. Distributions as a function of angles ϕ are obtained by deconvolution of these BES using Gaussian functions located at each ionization energy in the BES. The widths of the Gaussian functions can be determined from a consideration of published PES vibronic manifolds and the instrumental energy resolution function (1.2 eV FWHM). For each ionization process, the area of fitted peak is plotted as a function of momentum (calculated from using Eq. (1)). The set of areas as a function of momentum for a specific binding energy is referred to as an experimental momentum profile or XMP. To compare the XMPs with the relative cross-sections calculated as a function of momentum using expressions (2) and (3) above, the effects of the finite spectrometer acceptance angles in both θ and ϕ ($\Delta\theta \approx \pm 0.7°$ and $\Delta\phi \approx \pm 1.9°$) must be included. This is achieved in the present Letter with the Gaussian method [14].

The gaseous sample of propene measured in this Letter was 99.5% of purity and was used directly without further purification. No impurities were observed in the binding energy spectra.

3. Results and discussion

Propene has C_s point group symmetry and its electronic configuration in the ground state can be written as

$$(\mathrm{core})^6 \underbrace{(4a')^2(5a')^2(6a')^2}_{\text{innervalence}} \underbrace{(7a')^2(1a'')^2(8a')^2(9a')^2(10a')^2(2a'')^2}_{\text{Outervalence}}$$

In the ground state, the 24 electrons are arranged in 12 double-occupied orbitals in the independent particle description. All the molecular orbitals are either A′ or A″ symmetry. The PES of propene has been investigated extensively both experimentally and theoretically, such as HeI PES, HeII PES, X-ray PES, and synchrotron radiation PES reported [8–11], respectively. The assignment of the order of occupation for these valence orbitals, both from the PES experiments and the molecular orbital calculations, has been discussed in [15,11]. Peak ordering of 8a′ and 1a″ is reversed in the theoretical calculations in [8–10], while more accurate multi-reference

singles and doubles configuration interaction (MRSDCI) theoretical calculation gave the ordering as shown above [11].

To obtain the experimental momentum profiles, the BES were grouped according to different ϕ angles with a step 1°. The valence shell BES of propene for measurements at the azimuthal angle $\phi = 0°$ and $\phi = 7°$ are shown in Fig. 1. The binding energy spectra were fitted with a series of individual Gaussian peaks whose widths are combinations of the EMS instrumental energy resolution and the corresponding Franck–Condon widths derived from high-resolution PES data, and the relative energy values were given by the high-resolution PES. The fitted Gaussian curves for individual peaks are indicated by dotted lines, while their sum of overall fitted spectra are represented by the solid lines.

The binding energy for each valence orbital is obtained from PES data. In the PES work, the vertical ionization potential of the 2a″ HOMO was 10.03 eV, and the 10a′, 9a′, 8a′, 1a″, 7a′, 6a′, 5a′ and 4a′ orbitals were determined to be 12.31, 13.23, 14.48, 15.0, 15.9, 18.4, 22.1 and 23.9 eV, respectively.

In the present EMS work, 11 structures can be identified in the BES of Fig. 1. The vertical ionization potential of HOMO 2a″ is determined to be 10.03 eV. The vertical ionization potentials of the 10a′ and 7a′ are determined to be 12.3 and 13.3 eV, respectively, and the 6a′, 5a′ and 4a′ inner valence orbitals are determined to be 18.4, 22.1 and 23.9 eV, respectively. Since the energy separation between 8a′ and 1a″ is only 0.52 eV, an averaged ionization potential of 8a′ + 1a″ was given to be 14.6 eV. Some spectroscopic strength over 25 eV was observed and two Gaussian peaks with much broader FWHM were used to approximate their sum intensity. It is due to that that there are many satellite peaks with a smaller energy separation at this energy region, and EMS cannot tell them apart. The spectroscopic strength above 25 eV is mainly due to correlation effects in the target or in the final state of residual ion. To describe well the experimental binding energy spectra, the Gaussian peak at 20.3 eV indicated by 'a' must be included, otherwise the experimental intensity at the region of around 20.3 eV will be greatly underestimated, which is also identified by MRSDCI calculation in [11]. The differences in FWHMs of these peaks are due to the vibrational broadening of the lines.

The experimental momentum profiles (XMPs) were extracted by deconvolution of the same peak from the BES at different azimuthal angles. As is shown in Fig. 2, the XMPs of propene HOMO 2a″ with the impact energy of 1200 and 600 eV are compared with various theoretical momentum profiles (TMPs). It should be noted that the experimental instrumental angular resolutions have been incorporated in the calculations. The slight difference between TMPs at 1200 and at 600 eV is due to that the experimental momentum resolution becomes better at a lower impact energy. The small basis sets HF calculations (6-31G and STO-3G, curves 5 and 6, respectively) give poor predictions of the HOMO electron momentum distribution, especially in the low momentum region (below 1.0 a.u.). The 6-311++G** and AUG-CC-PVTZ HF and DFT calculations (curves 1, 2, 3 and 4) well describe the experimental result in general. However, in the regions of momentum <0.3 and >1.3 a.u., there is discernable discrepancy between XMPs and TMPs. A possible explanation for this is the distorted wave effects. Generally, higher momentum transfer is contributed from the electron in nearer

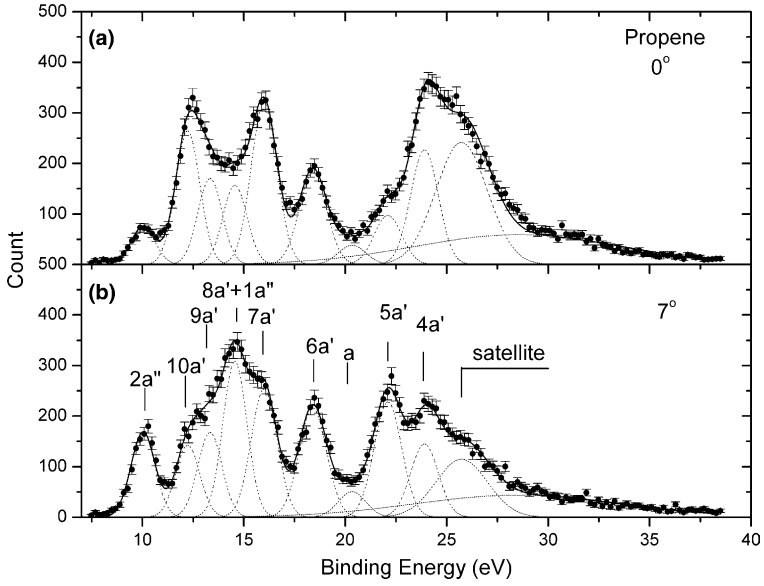

Fig. 1. Binding energy spectra of propene at $\phi = 0°$ (a) and $\phi = 7°$ (b) with 1200eV impact energy. The dashed and solid lines represent individual and summed Gaussian fits, respectively.

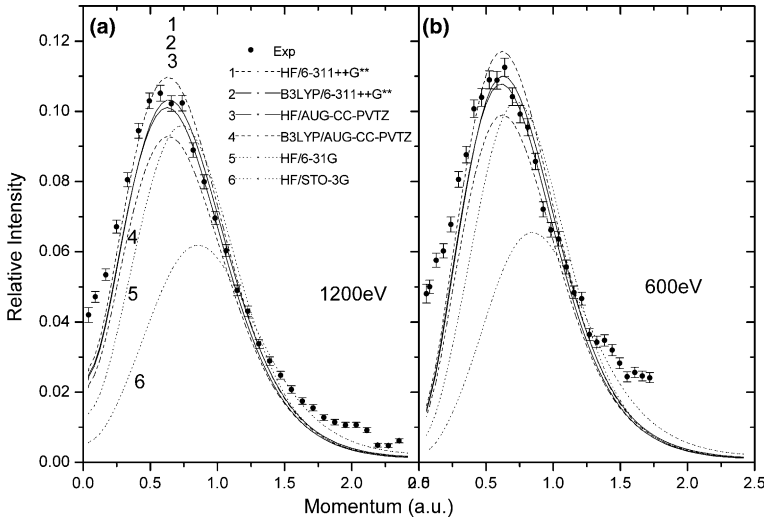

Fig. 2. Experimental and calculated momentum distributions for HOMO 2a″ orbital of propene with 1200 eV (a) and 600eV (b) impact energy. The theoretical momentum profiles are calculated using Hartree–Fock (curves 1, 3, 5 and 6) and DFT-B3LYP (curves 2 and 4) methods with the AUG-CC-PVTZ, 6-311++G**, 6-31G and STO-3G basis sets.

nucleus region and lower momentum from further nucleus region, so the distortion will become more evident at higher momentum. Nevertheless, the smaller momentum transfer might also come from the nearer nucleus region in some d-like orbitals, such as π* orbital [16–19], because the momentum is related to the gradient of the position space wavefunction: low momentum is consistent with the low gradient of the position space wavefunction. For d-like orbitals, the gradient of wavefunctions is very low in the region near the nucleus [19]. So the distorted wave effects will manifest more remarkably at lower momentum for d-like orbitals. The theoretical calculation shows that there is some extent π* orbital in the propene HOMO 2a″. To confirm this explanation, the experiment was carried out again at 600 eV. It is expected that the discrepancy will become more evident than that of 1200 eV because the nucleus will distort the electron waves greater at lower impact energy. Consequently, it is found that the turn-up is larger at 600 eV than at 1200 eV both in the region of momentum <0.3 and >1.3 a.u. as illustrated in Fig. 2a and b. The difference between experimental and B3LYP/6-311++G** theoretical intensity, for example, at 0.05 a.u. is 0.033 for 600 eV, while 0.017 for 1200 eV. So, the distorted wave effect explanation predicts well the experimental trends. The quantitative calculation for distorted wave effects in molecular orbital is still a challenge for theorists by far because of the multi-center system.

4. Conclusion

In summary, we report the first measurements of the complete valence shell BES and momentum profile for propene HOMO by EMS at the impact energy of 1200 and 600 eV. The experimental results are well described by associated theoretical calculations in general. The observable discrepancy between experimental and theoretical momentum profile in the regions of momentum <0.3 and >1.3 a.u. is explained qualitatively with the distorted wave effects. Since the frontier HOMO is particularly important for chemical reactivity and possibly molecular recognition from the pioneering work by Fukui [20] on frontier orbital theory, the chemical reaction for propene as a reactant molecule will increasingly benefit from the experimental and theoretical HOMO electron density distributions.

Acknowledgments

Project supported by the National Natural Science Foundation of China under Grant Nos. 19854002, 19774037 and 10274040 and the Research Fund for the Doctoral Program of Higher Education under Grant No. 1999000327.

References

[1] I.E. McCarthy, E. Weigold, Rep. Prog. Phys. 54 (1991) 789.
[2] M.A. Coplan, J.H. Moore, J.P. Doering, Rev. Mod. Phys. 66 (1994) 985.
[3] E. Weigold, I.E. McCarthy, Electron Momentum Spectroscopy, Kulwer Academic Plenum Publishers, New York, 1999.
[4] D.L. Cooper, N.L. Allan, J. Am. Chem. Soc. 114 (1992) 4773.
[5] B.P. Hollebone, J.J. Neville, Y. Zheng, C.E. Brion, Y. Wang, E.R. Davidson, Chem. Phys. 196 (1995) 13.
[6] J.K. Deng, G.Q. Li, X.D. Wang, et al., J. Chem. Phys. 117 (2002) 4839.

[7] J.K. Deng, G.Q. Li, J.D. Huang, et al., Chem. Phys. Lett. 313 (1999) 134.
[8] K. Kimura, S. Katsuwata, Y. Achiba, T. Yamazaki, S. Iwata, Handbook of HeI Photoelectron Spectra of Fundamental Organic Molecules, Halsted Press, New York, 1981.
[9] G. Bieri, F. Burger, E. Heilbronner, J.P. Maier, Helv. Chim. Acta 60 (1977) 2213.
[10] C. Liegener, S. Svensson, H. Agren, Chem. Phys. 179 (1994) 313.
[11] A.D.O. Bawagan, S.J. Desjardins, R. Dailey, E.R. Davidson, J. Chem. Phys. 107 (1997) 11.
[12] J.K. Deng, G.Q. Li, Y. He, et al., J. Chem. Phys. 114 (2001) 882.
[13] P. Duffy, D.P. Chong, M.E. Casida, D.R. Salahub, Phys. Rev. A 50 (1994) 4704.
[14] J.N. MiGdall, M.A. Coplan, D.S. Hench, et al., Chem. Phys. 57 (1981) 141.
[15] G. Fronzoni, G. DeAlti, P. Decleva, A. Lisini, Chem. Phys. 195 (1995) 171.
[16] J. Rolke, Y. Zheng, C.E. Brion, et al., Chem. Phys. 244 (1999) 1.
[17] J.K. Deng, G.Q. Li, J.D. Huang, et al., Chin. Phys. Lett. 19 (2002) 47.
[18] G.L. Su, C.G. Ning, S.F. Zhang, et al., Chem. Phys. Lett. 390 (2004) 162.
[19] C.E. Brion, Y. Zheng, J. Rolke, et al., J. Phy. B: At. Mol. Opt. Phys. 31 (1998) L223.
[20] K. Fukui, Angew. Chem., Int. Ed. Engl. 21 (1982) 801.